Renewable Energy 58 (2013) 85–94

Contents lists available at SciVerse ScienceDirect

Renewable Energy

journal homepage: www.elsevier.com/locate/renene

Reactive power management of distribution networks with wind generation for improving voltage stability

N.K. Roy [a,*], H.R. Pota [a], M.J. Hossain [b]

[a] School of Engineering and IT, The University of New South Wales, Canberra, ACT 2600, Australia
[b] Griffith School of Engineering, Griffith University, Gold Coast, QLD 4222, Australia

ARTICLE INFO

Article history:
Received 15 November 2012
Accepted 25 February 2013
Available online 9 April 2013

Keywords:
Composite load
Distributed generation
D-STATCOM
Q-loadability
Reactive power margin
Wind turbine

ABSTRACT

This paper proposes static and dynamic VAR planning based on the reactive power margin for enhancing dynamic voltage stability of distribution networks with distributed wind generation. Firstly, the impact of high wind penetration on the static voltage stability of the system is analysed and then the effect of composite loads on system dynamics is presented through an accurate time-domain analysis. A new index, reactive power loadability (*Q*-loadability), is used to measure the vulnerability of the network to voltage collapse. Compensating devices are located using *Q*-loadability to increase the system voltage stability limit. Finally, a cost-effective combination of shunt capacitor bank and distribution static compensator (D-STATCOM) is determined through static and dynamic analyses to ensure voltage stability of the system after a sudden disturbance for different wind penetration levels. This study takes into account the induction motor dynamic characteristics which influence the transient voltage recovery phenomenon. The results show that the proposed approach can reduce the required sizes of compensating devices which, in turn, reduces costs. It also reduces power losses and improves the voltage regulation of the system.

1. Introduction

In recent years, distributed generation (DG) has attracted strong interest because of economic and environmental factors. Its potential benefits include improved system reliability, reductions in greenhouse gas emissions and energy losses, and increased flexibility in investments [1]. However, the increased penetration of DG presents a significant challenge to distribution network operators as traditional distribution networks were generally not designed to connect power generation facilities. DG integration in these passive networks will add a new dynamic element due to the variability and uncertainty inherent in the operation of renewable energy sources. In this context, it is very important to understand the behaviour of DG-integrated systems to facilitate the overall planning of power distribution systems [2,3].

The load of a distribution network is always changing due to variations in consumer demands. In certain industrial areas, it has been observed that under certain critical loading conditions, the distribution system experiences voltage collapse [4]. The connection of a generator to the distribution system affects the flow of power and voltage profile of the system and the profiles are different for different types of loads [5]. The importance of load characteristics in power system simulation studies is highlighted by the IEEE Task Force in Ref. [6].

The main classification of loads is into static and dynamic types. Static loads can be classified as constant impedance, constant current and constant power loads. The modelling of loads is complicated because a typical load bus represented in a stability analysis is composed of a large number of devices, such as fluorescent and incandescent lamps, refrigerators, heaters, compressors, motors, furnaces, etc. The exact composition of a load is difficult to estimate as the load magnitude and composition vary greatly with location, temperature, time of day, season, etc. In power flow studies, the common practice is to represent the load characteristics as seen from power delivery points [7]. Most conventional load flows use a constant power load model in which it is considered that active and reactive powers are independent of voltage magnitudes. In distribution systems, nodal voltages vary widely as most of the buses are not voltage controlled [8]. Therefore, the load characteristics are important for distribution systems analysis.

Due to the integration of DG, distribution networks are becoming active systems where generation and load nodes are

* Corresponding author. Tel.: +61 2 626 88193; fax: +61 2 626 88443.
E-mail addresses: n.roy@student.unsw.edu.au (N.K. Roy), h.pota@adfa.edu.au (H.R. Pota), j.hossain@griffith.edu.au (M.J. Hossain).

0960-1481/$ – see front matter © 2013 Elsevier Ltd. All rights reserved.
http://dx.doi.org/10.1016/j.renene.2013.02.030

mixed. The interaction between generators and load characteristics affects the operation of distribution systems and proper reactive power planning is required as it is directly related to the voltage level control of distribution networks. This important issue has attracted much less attention in the available literature. Most of the papers in distribution systems have analysed the impact of DG penetration in the system considering static load models [9–11]. Static load models are not accurate enough for capturing all the dynamics of a network. In reality, distribution networks have composite loads which are composed of both static and dynamic elements. As loads are closer to the DG, the interaction between them is direct. This situation may require high dynamic compensation to ensure fast voltage recovery under post-fault condition.

Of the different dynamic compensating devices available, the static synchronous compensator (STATCOM) is increasingly being used to enhance dynamic voltage stability of the system [12]. However, the performance of a STATCOM depends upon its controller parameters and suitable location in the power network. Power quality and voltage stability of the system can be ensured using distribution static compensator (D-STATCOM) in low voltage (LV) grids with distributed energy resources (DERs) [9,13]; but in Refs. [9,13], a strategy for placing compensating devices with the new generation in distribution networks is not provided. A STATCOM with a suitable control has the potential to significantly increase the transient stability margin as well as voltage stability of a system [14]. However, it is an expensive device and should not be used without proper planning. Fuzzy logic based reactive power compensation planning for radial distribution feeders is proposed in Ref. [15]. But the analysis is carried out for only a shunt capacitor bank which cannot ensure dynamic voltage recovery. The reactive power delivered by the shunt capacitor is proportional to the square of the terminal voltage, which means that during low voltage conditions VAR support drops, thereby compounding the problem [16]. This situation may become worse when static load models are replaced by composite ones. A multi-objective approach for reactive power planning with wind generators is proposed in Ref. [17]. The methodology proposed in Ref. [17] determines the optimal location of, and reactive power injection from, static VAR compensator (SVC) sources in order to improve system's static voltage profile and power loss. However, the dynamic voltage stability issue is not considered in Ref. [17]. In our previous work [18], due to the lack of adequate placement planning, a large D-STATCOM was required to improve the dynamic voltage profile of distribution networks with constant PQ loads.

The main aim of this paper is to enhance the dynamic voltage stability of distributed generation systems in a cost-effective way which complies with industry standards. The effect of load models in distributed generation planning is demonstrated through nonlinear simulations. A new index, reactive power loadability (Q-loadability), is used to determine the best location for the D-STATCOM to enhance voltage stability. Both static and dynamic analyses are carried out to determine its required size. The parameters of the controller are also tuned to reduce the D-STATCOM's rating.

The remainder of this paper is organised as follows. In Section 2, the background of the proposed methodology is given. Section 3 presents the system description. Simulation results showing the impact of high wind penetration and different load characteristics on the system voltage stability are given in Section 4. The proposed planning approach is demonstrated in Section 5. The effectiveness of the proposed methodology is investigated through several case studies in Section 6 and the paper concludes with brief remarks in Section 7.

2. Background

Voltage stability is the ability of a power system to maintain steady acceptable voltages at all buses under both normal and abnormal (such as following a disturbance) operating conditions [16]. The main factor causing voltage instability is the inability of power systems to meet the demand of reactive power. In power systems, P–V (MW margins) and Q–V curves (MVAr margins) are used to determine the ability of a system to maintain voltage stability under normal and abnormal conditions. The P–V and Q–V curves are obtained through a series of AC power flow solutions [19]. The P–V curve is a representation of voltage changes as a result of an increased power transfer between two systems and the Q–V curve is a representation of reactive power demand by a bus or buses as voltage level changes.

The power flow relationship between the source and load can be illustrated by considering the simple radial network shown in Fig. 1 which consists of a constant voltage source (V_s) supplying a load (Z_{load}) through a series impedance (Z_{line}) [16].

The expression for current in Fig. 1 is

$$\tilde{I} = \frac{\tilde{V}_s}{\tilde{Z}_{line} + \tilde{Z}_{load}}, \tag{1}$$

where $\tilde{I}$ and $\tilde{V}_s$ are phasors, $\tilde{Z}_{line} = Z_{line}\angle\theta$, $\tilde{Z}_{load} = Z_{load}\angle\phi$. The magnitude of the current is

$$I = \frac{V_s}{\sqrt{(Z_{line}\cos\theta + Z_{load}\cos\phi)^2 + (Z_{line}\sin\theta + Z_{load}\sin\phi)^2}}, \tag{2}$$

which may be expressed as

$$I = \frac{V_s}{\sqrt{F}Z_{line}}, \tag{3}$$

where

$$F = 1 + \left(\frac{Z_{load}}{Z_{line}}\right)^2 + 2\left(\frac{Z_{load}}{Z_{line}}\right)\cos(\theta - \phi). \tag{4}$$

The magnitude of the receiving end voltage is given by

$$V_r = Z_{load}I = \frac{V_s Z_{load}}{\sqrt{F}Z_{line}}, \tag{5}$$

and the power supplied to the load is

$$P_r = V_r I\cos\phi = \left(\frac{Z_{load}}{F}\right)\left(\frac{V_s}{Z_{line}}\right)^2\cos\phi. \tag{6}$$

The loading of the network can be increased by decreasing the value of Z_{load}. For P–V analysis, the loading of the network is

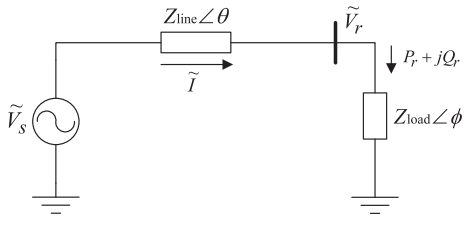

Fig. 1. A simple radial distribution system.

increased with V_s, load power factor and line parameters fixed. From Eq. (6), as Z_{load} is decreased gradually the load power, P_r, increases, hence the power transmitted increases. As the value of Z_{load} approaches Z_{line}, the value of P_r starts to decrease gradually due to F. From Eq. (5), it is seen that as Z_{load} decreases, the receiving end voltage V_r decreases gradually. The plot of the relationship between V_r and P_r as the power transfer is increased due to increased loading gives the P–V curve which demonstrates the effect of active power flow on voltage instability. However, from Eqs. (5) and (6), it is seen that the power factor of the load has a significant impact on the overall equations. This is to be expected because the voltage drop in the line is a function of active as well as reactive power transfer. Hence, Q–V curves can be used to assess voltage stability of the system. The suitability of Q–V analysis compared to P–V analysis is investigated in Ref. [20] which states that Q–V curves can be used to identify critical nodes in a distribution system with all kinds of load uncertainties. Our focus in this paper, therefore, is on the Q–V analysis.

2.1. Q–V method

Starting with the existing reactive loading at a bus, the voltage of the bus can be computed for a series of load flows with the increasing reactive load. The bus voltage magnitude increases as the reactive power injected at the same bus is increased. When the voltage of any bus decreases with an increase in the reactive power for that bus, the system is said to be unstable. The reactive power margin (Q-margin) is measured as the distance between the lowest MVAr point of the Q–V curve and the voltage axis, as shown in Fig. 2 [19]. A higher Q-margin signifies a stronger bus and a lower one signifies a weaker bus. The standard procedure for conducting voltage collapse analysis based on Q–V curves is as follows:

1. establish a power flow case;
2. choose a load bus which could be a load that is suspected or known to be susceptible to voltage collapse;
3. increase the reactive power by 0.1 pu at the chosen bus, note that except this change, nothing else changes in the data;
4. solve the power flow program with this change;
5. record the bus voltage (V) and reactive power (Q);
6. iterate Step 3 until the power flow ceases to converge;
7. run the program that plots the Q–V curve using the recorded V and Q; and
8. compute the Q-margin from the Q–V curve.

To determine the suitable location for compensating devices, the increment in the Q-loadability is calculated using the following equation.

$$\%Q\text{-loadability} = \frac{Q\text{-margin}_{new} - Q\text{-margin}_{old}}{Q\text{-margin}_{old}} \times 100, \quad (7)$$

where Q-margin$_{old}$ and Q-margin$_{new}$ refer to the Q-margins of the bus before and after connection of the compensating device, respectively. In this paper, the Q-loadability is used as an index to measure the vulnerability of the network, with higher values of it signifying that the system is less vulnerable to voltage collapse.

3. System description

To simulate and analyse a system under various circumstances, a test system is essential. In this paper, Kumamoto 15-bus distribution test system shown in Fig. 3 [21] is considered. A wind generator is connected at bus 13, bus 1 is connected to the grid and a fixed capacitor equal to one-third of the generator's capability is connected at the terminal of the wind generator to provide the reactive power needed to operate it [22]. The total load on the system is 6.301 MW, 0.446 MVAr. Distribution system lines are modelled as $R + jX$. The machine parameters and test system data with loads are given in the Appendix.

The nonlinear model of the wind turbine used in this paper is based on a static model of aerodynamics, with a two-mass model of a drive train and a third-order model of an induction generator [23].

The D-STATCOM shown in Fig. 4 consists of a voltage source converter (VSC) connected to a DC capacitor. By controlling the firing angle of the VSC, reactive power can be either supplied from or absorbed by the D-STATCOM and thus, voltage regulation (VR) can be achieved. The dynamics for the D-STATCOM can be described by the following equation:

$$\dot{v}_{dc}(t) = -\frac{P_s}{Cv_{dc}} - \frac{v_{dc}}{R_C C}, \quad (8)$$

where v_{dc} is the capacitor voltage, C is the DC capacitor, R_C is the internal resistance of the capacitor, $E = kv_{dc}\angle\alpha$, where α is the bus angle of the D-STATCOM, k is the constant associated with the inverter of the D-STATCOM and P_s is the power supplied by the system to the D-STATCOM to charge the capacitor. The terminal

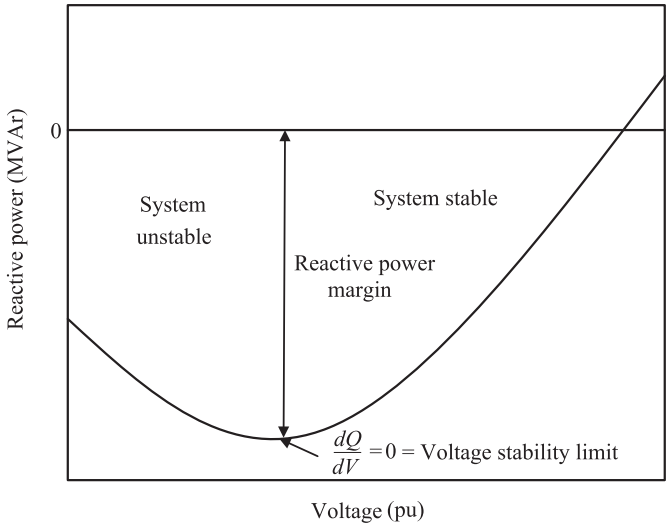

Fig. 2. Typical reactive power–voltage (Q–V) curve.

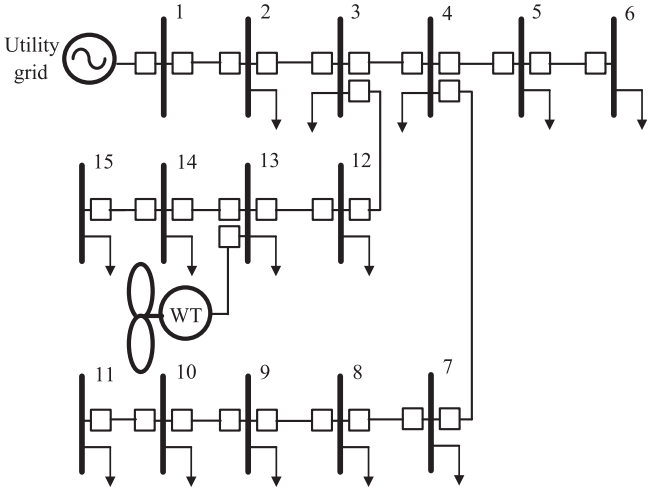

Fig. 3. Single line diagram of Kumamoto 15-bus distribution system.

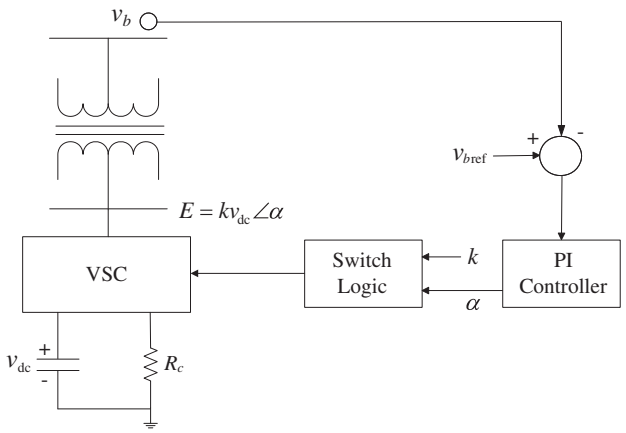

Fig. 4. D-STATCOM equivalent circuit and control.

voltage of the D-STATCOM is measured using a transducer with a first-order dynamics [18]. In this paper, k is fixed and α is used as the control variable.

In this paper, the load components are aggregated based on the IEEE Task force report [24] which assumes that a load delivery point consists of 30% static loads (space heating, cooking, water heater, etc.), 20% fluorescent lighting and 50% induction motors. The active components of static loads are represented by constant current models and the reactive components by constant impedance models, as recommended in [6] for dynamic simulations. An exponential load model is used for fluorescent lighting with the exponents a and b equal to 1 and 3, respectively [19] and a third-order model is used to represent aggregated residential motor loads [25]. An example of the composite load model representation used in this paper is shown in Fig. 5.

The impact of different load models and wind generator integration in the distribution network using the above models are discussed in the next section.

4. Impact study

The impact study of distribution systems identifies the changes required in the system design, equipment and operation to most effectively accommodate renewable energy. Impacts of large scale wind integration and load characteristics on the system voltage stability are described below.

4.1. Impact of high wind penetration

In order to observe the impact of high wind penetration, Q–V analysis is performed for different penetration levels. The Q-margins

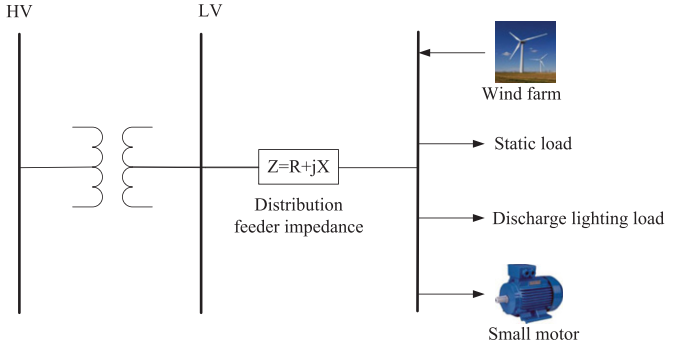

Fig. 5. An example of composite load with DG.

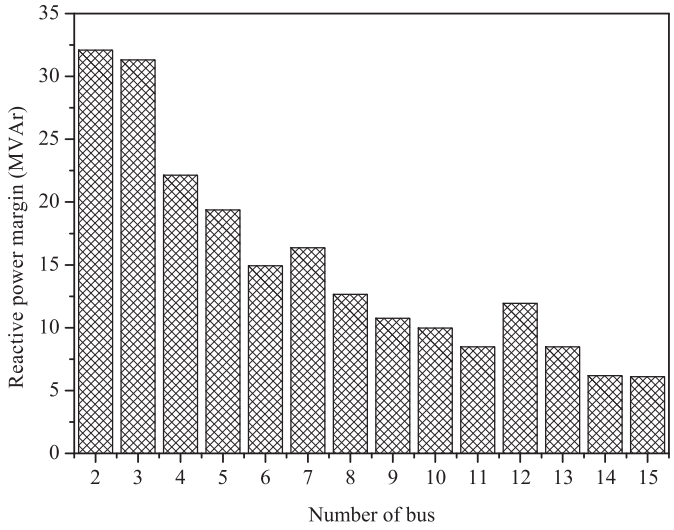

Fig. 6. Reactive power margins of the load buses in the test system for the base case (without wind generator).

of the load buses in the 15-bus test system for the base case are shown in Fig. 6. It can be observed that bus 15, which has the lowest Q-margin, is the weakest while, on the other hand, as bus 2 has the highest Q-margin, it is the strongest and the next 4 weak buses are 14, 13, 11 and 10. In this paper, wind generator is intentionally placed in the weak region at bus 13 to simulate the worst-case scenario. Q-margins for increasing wind penetration levels are given in Table 1 in which it can be seen that higher penetrations reduce the static voltage stabilities of the load buses, thereby increasing the possibility of voltage collapse.

To investigate the wind generator interaction with the system, eigenvalues are also calculated. The eigenvalue analysis shows that the dominant mode of the system with the composite load is monotonic. The dominant mode as a function of the wind penetration level is shown in Fig. 7. From this figure, it can be observed that the system is stable for low penetrations of wind but becomes unstable at high penetration levels.

4.2. Impact of load characteristics on voltage stability

Static and composite load models are used in this study to compare their impact on voltage stability. For the dynamic analysis, the system is tested with a sudden three-phase short-circuit fault at

Table 1
Reactive power margins for different wind penetration levels.

Bus no.	Q-margin (MVAr)				
	0%	30%	50%	80%	100%
2	32.10	30.71	29.02	24.75	22.06
3	31.31	29.92	28.24	24.07	21.48
4	22.13	21.47	20.79	19.11	17.59
5	19.38	18.86	18.34	17.14	16.01
6	14.93	14.57	14.24	13.54	12.91
7	16.36	15.95	15.56	14.71	13.95
8	12.65	12.36	12.09	11.55	11.08
9	10.76	10.52	10.31	9.88	9.52
10	9.98	9.76	9.57	9.18	8.86
11	8.48	8.30	8.14	7.83	7.57
12	11.93	10.75	9.71	8.82	8.02
13	8.48	8.31	7.99	7.73	7.62
14	6.19	5.66	5.22	4.41	3.80
15	6.10	5.59	5.16	4.37	3.78

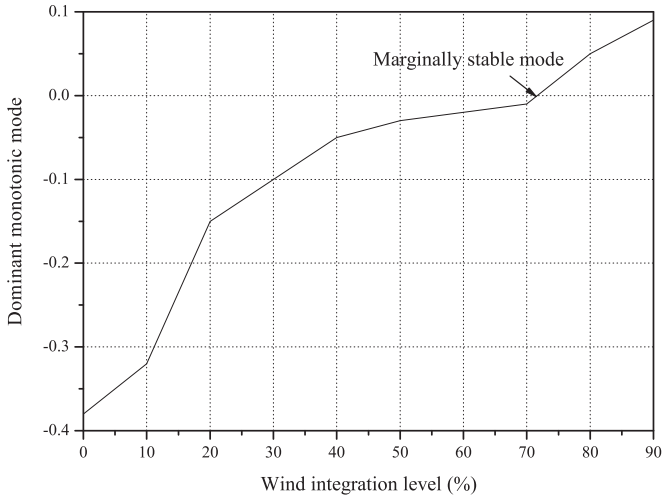

Fig. 7. Monotonic mode as a function of wind penetration level with the composite load.

bus 2 with 50% wind penetration. A three-phase short-circuit fault is applied at 1 s and cleared at 1.15 s. Fig. 8 shows the voltages at the point of common coupling (PCC) for constant impedance, constant current, constant power and composite loads. It illustrates that the system with static loads is less affected by a short-circuit fault than that with the composite load. According to IEEE Std. 1547 [26,27], voltage of distribution networks should recover to an acceptable level within the time indicated in Table 2. It can be seen that the system with the composite load takes a much longer than the permitted time of 2 s to return to its pre-fault condition. The load dynamics slow down the voltage recovery process and it requires the integration of dynamic compensating devices to meet the grid standard. The speed deviation of the wind generator for the composite load is shown in Fig. 9. Under the same fault condition for the composite load, the real and reactive power flow through the branch 1–2 is shown in Figs. 10 and 11, respectively. The post-fault oscillating powers are quite high for this branch and, if these values are higher than the threshold limits, the protective devices may react and isolate this system from the main grid.

The impact of high wind penetration is also investigated for the above faulted case with different load characteristics. From the

Table 2
Interconnection system response to abnormal voltages [26].

Voltage range (pu)	Clearing time (s)
$0 < 0.5$	0.16
$0.5 \leq V < 0.88$	2.00
$1.1 < V < 1.2$	1.00
$V \geq 1.2$	0.16

small-signal stability analysis (Fig. 7), it can be observed that, for 72% wind penetration, the system is marginally stable which may become unstable under a severe disturbance. The voltage profiles of the system at the PCC for 72% wind penetration under pre-fault, faulted and post-fault conditions are shown in Fig. 12. It can be clearly seen that, although the system maintains its stability for all types of static loads, it becomes unstable for the composite load. This is because induction motor loads draw very large reactive currents from the main grid during the voltage recovery which depresses the network's voltage profile. Therefore, an accurate load representation is essential for stability analyses of distribution networks; otherwise it can lead to different criteria regarding a system's stability.

5. Critical bus-oriented mixed VAR planning

A major factor contributing to voltage instability is the voltage drop that occurs due to the consumption of reactive power by inductive components of power networks [28]. Maintaining acceptable voltage levels within the specified times shown in Table 2 is an important objective of the present study. To improve the voltage recovery time for systems with composite loads, we need fast responsive dynamic compensating devices in proper places. Common industrial practice is to connect compensating devices at the PCC of the generators to the system. According to IEEE Std. 1547, DG units are not allowed to regulate voltage actively at the PCC [26]. Therefore, it is important to select a suitable bus for the installation of dynamic compensating devices to regulate the system voltage.

5.1. Selection of location

Although a suitable bus can be easily selected from the Q–V analysis with a compensating device connected to the bus, it is

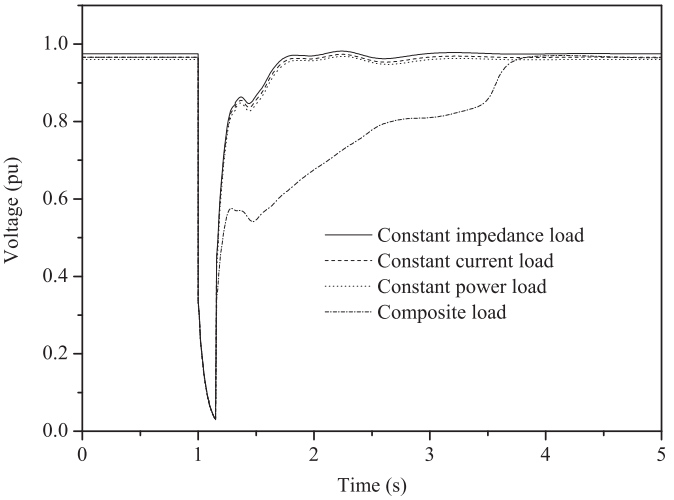

Fig. 8. Voltage at the PCC (bus 13) for different types of load models for 50% wind penetration (sudden three-phase fault at bus 2).

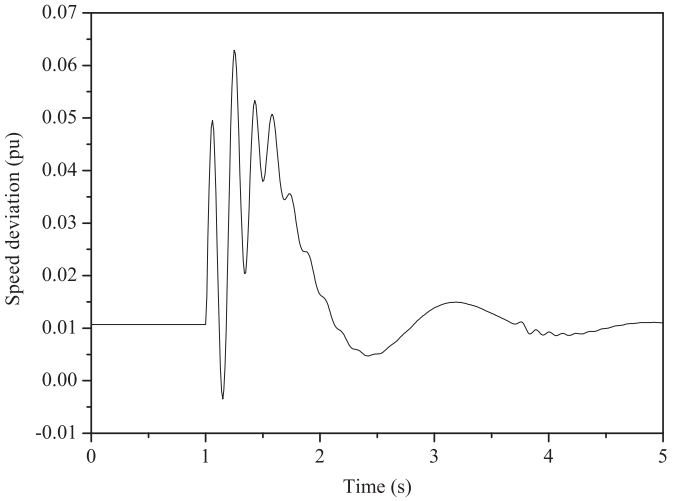

Fig. 9. Speed deviation of wind generator for the composite load (sudden three-phase fault at bus 2).

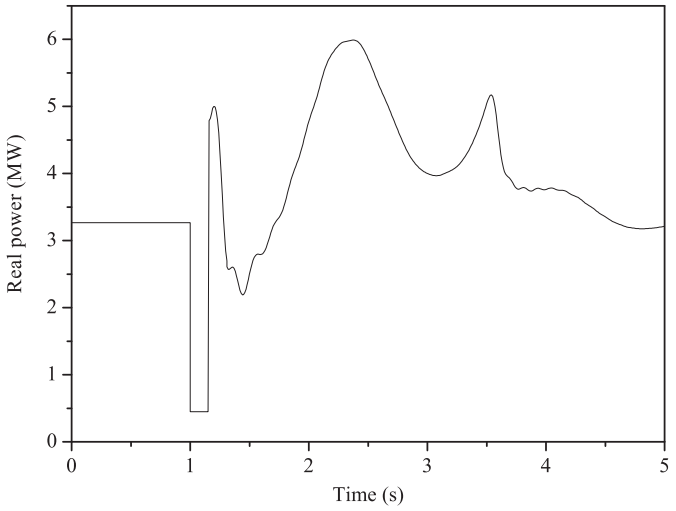

Fig. 10. Real power flow of branch 1–2 for the composite load (sudden three-phase fault at bus 2).

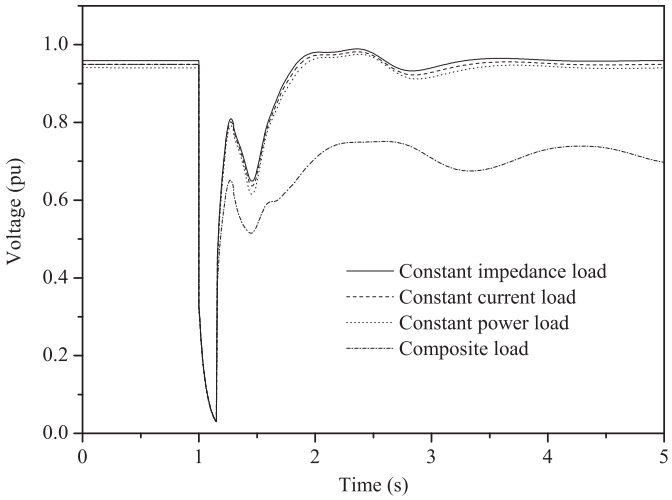

Fig. 12. Voltage at the PCC (bus 13) for different types of load models for 72% wind penetration (sudden three-phase fault at bus 2).

time-consuming to perform this analysis for each bus. Therefore, to reduce the computational burden, the same amount (2 MVAr) of reactive power source is connected to some of the candidate buses in the weak and strong regions to calculate the increments in *Q*-loadability from Eq. (7). For the strong and weak regions, candidate buses refer to those which have higher and lower Q-margins than others in those regions, respectively. The percentage increment in the *Q*-loadability is greater at the weak than strong buses and it is highest for the most critical bus (bus 15), as shown in Table 3. Therefore, to maximise the *Q*-loadability of the system and to reduce the possibility of voltage collapse, the weakest bus is a good choice to install the compensating device.

Fig. 13 shows the voltage profiles at the PCC for the composite load with and without the D-STATCOM placed at the critical bus. For comparison purposes, a simulation response is also plotted by connecting a D-STATCOM at the PCC. Table 4 shows the performances of the D-STATCOM for different connections in which it can be observed that, if we connect a D-STATCOM at the weakest bus, the system has fast voltage recovery time compared to its connection at the PCC. The reason is, if we can stabilise the most critical bus quickly, it can also ensure fast recovery time for the other buses. Moreover, the connection of a D-STATCOM at the weakest bus reduces the system's power loss by 16.88% compared with connecting it at the PCC and it can be seen that only a reduced-capacity (1.8 MVAr) D-STATCOM is needed to obtain a grid code compatible performance.

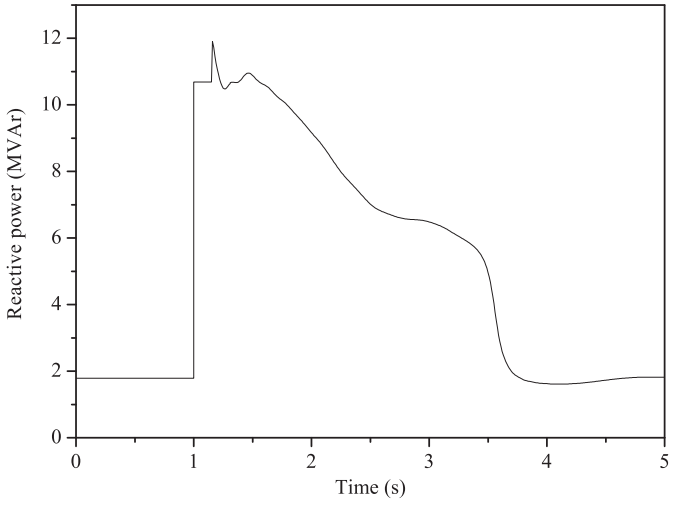

Fig. 11. Reactive power flow of branch 1–2 for the composite load (sudden three-phase fault at bus 2).

5.2. Determination of size for static and dynamic compensators

It is well-known that D-STATCOMs are quite expensive and, therefore, cannot be used extensively. The use of the smallest capacity dynamic compensating device to obtain the grid code compatible performance is also an important objective of this study. In this paper, a mixed (static and dynamic) VAR planning is performed to reduce the size of the D-STATCOM required to maintain voltage stability.

Static shunt capacitor banks have the advantage of being much cheaper than other devices that are generally used to support the reactive power. The sizes and costs of commercially available three-phase capacitors are given in Table 5. The sizes of D-STATCOMs in the market vary from 100 kVAr to 10 MVAr [29] and the cost is $50/kVAr [30]. Firstly, a random combination of a shunt capacitor and D-STATCOM is chosen from the available sizes. Then, through several load flow calculations and dynamic simulations, a cost-effective combination which can maintain the static and dynamic voltage profiles of the system according to the utility requirement is determined. It is seen that a D-STATCOM of less than 0.75 MVAr cannot ensure dynamic voltage recovery within 2 s after a sudden disturbance for 50% wind penetration. To maintain the steady-state voltage profile of all buses of the network in the range 0.95–1.05 pu [12], we also need a 1.05 MVAr capacitor with this D-STATCOM. This combination has a voltage recovery time of 1.56 s which is compatible with the grid code. For 72% penetration of wind the

Table 3
Reactive power loadabilities of weak and strong buses.

Weak bus		Strong bus	
Bus no.	*Q*-loadability (%)	Bus no.	*Q*-loadability (%)
15	10.27	2	1.92
14	9.93	3	1.97
11	6.10	4	2.40

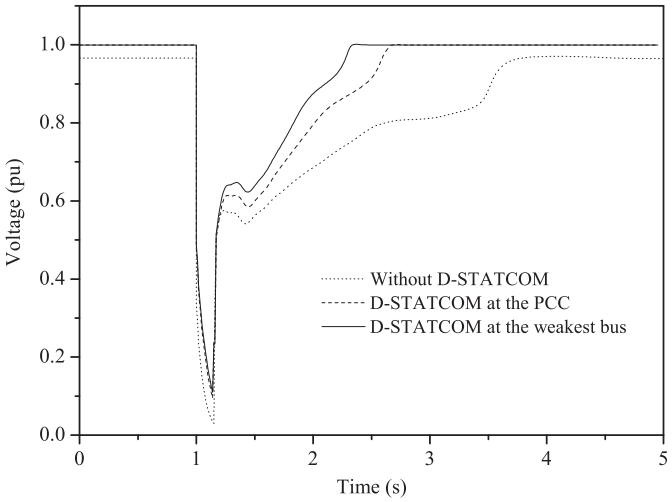

Fig. 13. Voltage at the PCC (bus 13) for connection of D-STATCOM in different places (sudden three-phase fault at bus 2).

recovery time is 1.72 s with a combination of 1.8 MVAr capacitor and 0.88 MVAr D-STATCOM. A flow-chart of the proposed VAR planning approach is shown in Fig. 14. Using the proposed approach, the voltages of the wind generator bus shown in Fig. 15 certainly maintain the grid code. In this study, the controller is chosen as

$$G_{PI}(s) = K_p\left(1+\frac{1}{T_i s}\right), \tag{9}$$

where K_p and T_i are the proportional-integral (PI) controller parameters. As the performance of a D-STATCOM depends on the proper tuning of the controller parameters, the gains of the PI controller are tuned using Ziegler–Nichols tuning method which is a widely used practical method to tune the controller parameters [31]. A proper tuning of the controller parameters results in a lower-rating D-STATCOM. The values of K_p and T_i along with the sizes of the compensating devices and voltage recovery times are given in Table 6 for different wind penetration levels.

6. Effectiveness of the proposed methodology

The purpose of this paper is to develop an effective methodology for reactive power compensation of distribution networks. The following results verify the effectiveness of the proposed VAR planning approach.

Table 4
Performances of D-STATCOM at the PCC and at the weakest bus.

Connection point	D-STATCOM capacity (MVAr)	Voltage at PCC (pu)	Recovery time (s)	Power loss (MW)
PCC	2.0	1.0	1.73	0.1427
Weakest bus (bus 15)	1.8	0.99	1.42	0.1186

Table 5
Available three-phase capacitor sizes and costs [15].

Size (kVAr)	150	300	450	600	900	1200
Cost (USD)	750	975	1140	1320	1650	2040

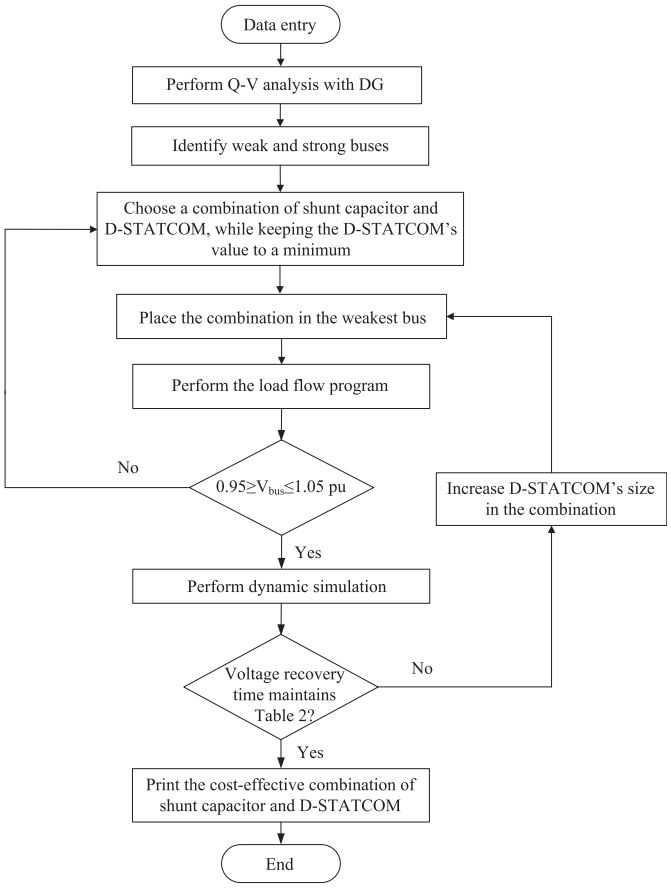

Fig. 14. Flow-chart of the proposed VAR planning scheme.

6.1. Effect on static voltage stability of the system

The main factor causing voltage instability is the inability of a power system to maintain a proper balance of reactive power throughout the system which is often associated with its reactive power generating sources being improperly located. As the weak buses are more vulnerable to voltage collapse, the *Q*-margins of the

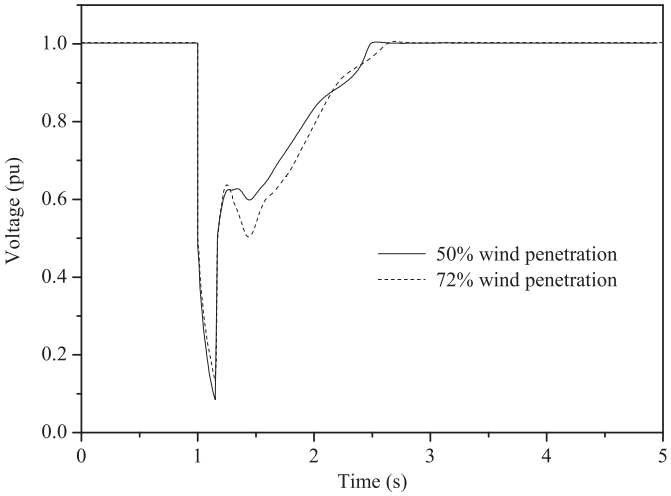

Fig. 15. Voltage at the PCC (bus 13) with the cost-effective combination of shunt capacitor and D-STATCOM (sudden three-phase fault at bus 2).

Table 6
Controller parameters, device sizes and recovery times for the proposed approach.

Wind penetration level	K_p	T_i	Shunt capacitor (MVAr)	D-STATCOM (MVAr)	Voltage recovery time (s)
30%	3.11	1.62	0.90	0.40	1.40
50%	5.20	1.45	1.05	0.75	1.56
72%	6.60	1.35	1.80	0.88	1.72
80%	6.63	1.36	1.80	0.90	1.79
100%	6.97	1.12	2.25	1.30	1.86

weak regions are calculated through several load flow studies. It is seen that placing the D-STATCOM at the critical bus increases the stability margin of the load buses compared to its connection at the PCC. The *Q*-margins of the weak areas are given in Table 7 which signify that proper placement of the D-STATCOM can accommodate more wind energy without greatly reducing system stability.

6.2. Effect on steady-state VR

Power distribution systems are dominated by loads. The load components of a system are always switching in and out due to consumers' usage. It is desirable that steady-state VR, i.e., the difference in a system's voltage profile between maximum and minimum demand, should be as small as possible to ensure that all the electrical equipment connected to it works properly. Otherwise, the fluctuations in voltage can reduce the service life of the equipment or damage it. To ensure the security of the system, the following global voltage index is employed to quantify the VR [32]:

$$VR = \frac{1}{n}\sum_{i=1}^{n}|V_{\text{imax}} - V_{\text{imin}}| \times 100, \tag{10}$$

where n is the total number of buses, V_{imax} is the nodal voltage of bus i for maximum demand and V_{imin} is the nodal voltage of bus i for minimum demand. It is assumed that the maximum and minimum demands are ±10% above and below the system's nominal load, respectively.

The VRs are calculated from Eq. (10) for the connection of D-STATCOM in different locations which are presented in Table 8. The results demonstrate that the connection of the compensating device provides an acceptable VR in both cases, but that in our proposed approach is the minimum for all penetration levels.

6.3. Application of the proposed methodology on the widely used 16-bus test system

A 16-bus 3-feeder distribution test system [33], as shown in Fig. 16, is used to verify the effectiveness of the proposed methodology with multiple DG units. The total load on the system is 28.7 MW, 17.3 MVAr. Two wind generators, one at bus 2 and one at

Table 8
Steady-state voltage regulations for different wind penetration levels.

Connection point	VR (%)			
	30%	50%	80%	100%
D-STATCOM at PCC	1.80	1.76	1.73	1.68
Proposed approach	1.71	1.68	1.64	1.62

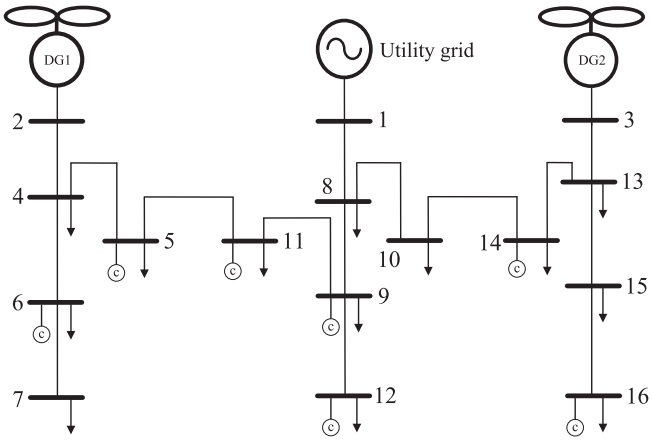

Fig. 16. Single line diagram of 16-bus distribution test system.

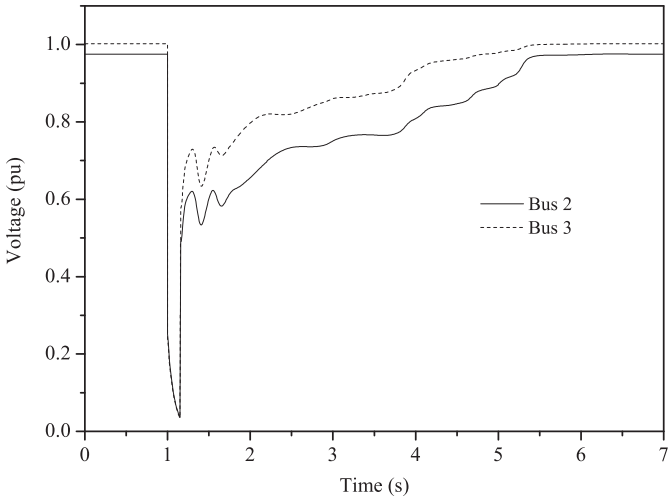

Fig. 17. Voltage at the PCC with the composite load (sudden three-phase fault at bus 8).

Table 7
Reactive power margins in the weak regions for different wind penetration levels.

Bus no.	*Q*-margin (MVAr)							
	30%		50%		80%		100%	
	D-STATCOM at PCC	Proposed approach	D-STATCOM at PCC	Proposed approach	D-STATCOM at PCC	Proposed approach	D-STATCOM at PCC	Proposed approach
10	9.90	9.91	9.86	9.87	9.72	9.74	9.59	9.60
11	8.42	8.43	8.40	8.40	8.37	8.38	8.26	8.26
13	8.40	8.42	8.31	8.32	8.20	8.23	8.05	8.09
14	6.11	6.15	5.67	5.70	5.11	5.15	5.01	5.04
15	5.93	5.98	5.60	5.64	5.06	5.12	4.98	5.01

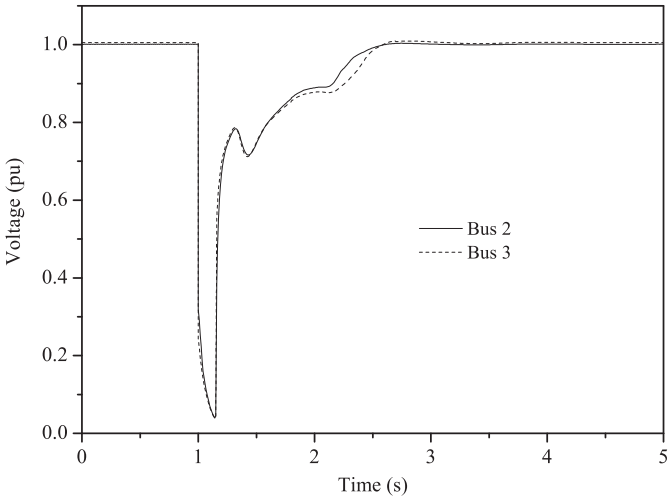

Fig. 18. Voltage at the PCC with the cost-effective combination of shunt capacitor and D-STATCOM (sudden three-phase fault at bus 8).

Table 9
Compensation required for 16-bus test system for the proposed and conventional approaches.

Approach	No. of D-STATCOMs required	Required capacity
Conventional	2 (at buses 2 and 3)	3.3 MVAr (at bus 2) + 2.75 MVAr (at bus 3)
Proposed	1 (at bus 7)	3 MVAr capacitor + 2.6 MVAr D-STATCOM

bus 3, are connected, each of which supports 50% of the system loads. The test system data with distributions of system loads in different nodes are given in Ref. [33].

The system voltage profiles with the composite load for a sudden three-phase fault at bus 8 are shown in Fig. 17 from which it can be clearly seen that the system takes a long time to return to its pre-fault condition following a disturbance. The Q–V analysis shows that bus 7 is the weakest bus and that connecting a combination of shunt capacitor and D-STATCOM there gives voltage recovery times of 1.61 s and 1.66 s for bus 2 and bus 3, respectively, as shown in Fig. 18. The required number of D-STATCOMs and their capacities for the proposed and conventional approach are summarised in Table 9 which shows that, for the proposed approach, a smaller single D-STATCOM is sufficient to maintain the system voltage within the acceptable level.

7. Conclusions

In this paper, the dynamic behaviour of distribution systems for different load models is investigated and an efficient reactive power planning scheme considering dynamic loads is proposed. The analysis shows that a high penetration of distributed wind generation reduces the voltage stability margin of the system. The load behaviour is found as one of the main driving forces of the voltage instability. Time-domain simulations demonstrate that the system with static load models returns to its pre-fault condition without violating grid constraints. However, that with composite load characteristics responds slowly to returning to its original state after a sudden disturbance and results in violation of the grid code. Therefore, it can be concluded that accurate load models play a very important role in dynamic voltage stability analyses of distribution systems and should be used when specifying any control or optimisation task. As a system's voltage stability depends on adequate reactive power support, the Q-margin, as an objective of increasing Q-loadability, can be used as a reliable index for the placement of the dynamic compensating device in a distribution network. Finally, it is evident that placing compensating devices at the critical location in the proper combination has the significant potential to enhance the voltage profile of a distribution network and reduce the system's power loss. This will prevent unnecessary disconnection of DG units by improving voltage stability of the system.

Although the proposed methodology is demonstrated for fixed-speed wind generators, it is applicable to any other generators connected to distribution networks because the Q-loadability index can be easily calculated for any power system. It is well-known that converter-connected wind turbines have their own reactive power regulation capabilities. However, by following some grid codes which strongly suggest operating DG units close to the unity power factor, the reactive power support from the generator will not be sufficient to cover the consumption of reactive power by loads following a disturbance. In this case, the proposed methodology is useful as it reduces the required size of the dynamic compensating device.

Acknowledgement

The authors would like to thank T. Aziz of the University of Queensland, Australia, for his valuable input.

Appendix

The machine parameters used for the system are given below:

Induction generator parameters:

Power = 2 MW, voltage = 690 V, frequency, $f = 50$ Hz, rated slip = 0.02, stator resistance, $R_s = 0.0121$ pu, stator reactance, $X_s = 0.0742$ pu, magnetising reactance, $X_m = 2.7626$ pu, rotor resistance, $R_r = 0.008$ pu, rotor reactance, $X_r = 0.1761$ pu.

Two-mass model parameters:

Inertia constant, $H_m = 2.6$ s, $H_g = 0.22$ s, torsion damping, $D_m = 3$ pu, $D_g = 0.6$ pu, torsion stiffness, $K_s = 141$ pu, gearbox ratio = 23.75.

Motor parameters:

Stator resistance, $R_{sm} = 0.077$ pu, stator reactance, $X_{sm} = 0.107$ pu, magnetising reactance, $X_{mm} = 2.22$ pu, rotor resistance, $R_{rm} = 0.079$ pu, rotor reactance, $X_{rm} = 0.098$ pu, inertia constant $H = 0.74$ s.

Table 10
Line and load data of 15-bus Kumamoto distribution system [21].

SE	RE	R (pu)	X (pu)	B (pu)	P_l (pu)	Q_l (pu)
1	2	0.003145	0.075207	0.00000	0.02080	0.0021
2	3	0.000330	0.001849	0.00150	0.04950	0.0051
3	4	0.006667	0.030808	0.03525	0.09580	0.0098
4	5	0.005785	0.014949	0.00250	0.04420	0.0045
5	6	0.014141	0.036547	0.00000	0.01130	0.0012
4	7	0.008001	0.036961	0.03120	0.06380	0.0066
7	8	0.008999	0.041575	0.00000	0.03230	0.0033
8	9	0.007000	0.032346	0.00150	0.02130	0.0022
9	10	0.003666	0.016940	0.00350	0.02800	0.0029
10	11	0.008999	0.041575	0.00200	0.21700	0.0022
3	12	0.027502	0.127043	0.00000	0.01320	0.0014
12	13	0.031497	0.081405	0.00000	0.00290	0.0003
13	14	0.039653	0.102984	0.00000	0.01610	0.0016
14	15	0.016070	0.004153	0.00000	0.01390	0.0014

Base power is 10 MVA and base voltage is 6.6 kV, SE and RE are the sending and receiving end nodes, respectively.

D-STATCOM parameters:

$C = 300\ \mu\text{F},\ \ R_c = 0.01$ pu.

The line and load data of 15-bus Kumamoto distribution system are given in Table 10.

References

[1] Ruiz-Romero S, Colmenar-Santos A, Gil-Ortego R, Molina-Bonilla A. Distributed generation: the definitive boost for renewable energy in Spain. Renewable Energy 2013;53:354–64.
[2] Kersting WH. Distribution system modeling and analysis. New York: CRC Press; 2006.
[3] Ding M, Zhang Y, Mao M. Key technologies for microgrids-a review. In: International conference on sustainable power generation and supply. Nanjing; 2009. p. 1–5.
[4] Chakravorty M, Das D. Voltage stability analysis of radial distribution networks. Electrical Power and Energy Systems 2001;23:129–35.
[5] Roy NK, Hossain MJ, Pota HR. Effects of load modeling in power distribution system with distributed wind generation. In: Australasian universities power engineering conference. Brisbane; 2011. p. 1–6.
[6] IEEE Task Force. Load representation for dynamic performance analysis. IEEE Transactions on Power Systems 1993;8(2):472–82.
[7] Mithulananthan N, Salama MMA, Caizares CA, Reeve J. Distribution system voltage regulation and var compensation for different static load models. International Journal of Electrical Engineering Education 2000;37(4):384–95.
[8] Haque MH. Load flow solution of distribution systems with voltage dependent load models. Electric Power Systems Research 1996;36:151–6.
[9] Freitas W, Asada E, Morelato A, Xu W. Dynamic improvement of induction generators connected to distribution systems using a DSTATCOM. In: Power system technology-PowerCon. Kunming; 2002. p. 173–7.
[10] Ravishankar J, Devi RPK. Effect of tuned unified power flow controller to mitigate the rotor speed instability of fixed-speed wind turbines. Renewable Energy 2009;34(4):591–6.
[11] Emhemed AS, Tumilty RM, Singh NK, Burt GM, McDonald JR. Analysis of transient stability enhancement of LV-connected induction microgenerators by using resistive-type fault current limiters. IEEE Transactions on Power Systems 2010;25(2):885–93.
[12] Lahaçani NA, Aouzellag D, Mendil B. Static compensator for maintaining voltage stability of wind farm integration to a distribution network. Renewable Energy 2010;35(11):2476–82.
[13] Wasiak I, Mienski R, Pawelek R, Gburczyk P. Application of DSTATCOM compensators for mitigation of power quality disturbances in low voltage grid with distributed generation. In: 9th international conference on electrical power quality and utilisation. Barcelona; 2007. p. 1–6.
[14] Hossain MJ, Pota HR, Ramos RA. Robust STATCOM control for the stabilisation of fixed-speed wind turbines during low voltages. Renewable Energy 2011;36(11):2897–905.
[15] Mekhamer SF, Soliman SA, Moustafa MA, El-Hawary ME. Application of fuzzy logic for reactive-power compensation of radial distribution feeders. IEEE Transactions on Power Systems 2003;18:206–13.
[16] Kundur P. Power system stability and control. New York: McGraw-Hill; 1994.
[17] Alonso M, Amaris H, Alvarez-Ortega C. A multiobjective approach for reactive power planning in networks with wind power generation. Renewable Energy 2012;37(1):180–91.
[18] Roy NK, Hossain MJ, Pota HR. Voltage profile improvement for distributed wind generation using D-STATCOM. In: IEEE PES general meeting. Detroit; 2011. p. 1–6.
[19] Taylor CW. Power system voltage stability. New York: McGraw-Hill; 1994.
[20] Aziz T, Saha TK, Mithulananthan N. Identification of the weakest bus in a distribution system with load uncertainties using reactive power margin. In: Australasian universities power engineering conference. Christchurch; 2010. p. 1–6.
[21] Li S, Tomsovic K, Hiyama T. Load following functions using distributed energy resources. In: IEEE power engineering society summer meeting. Seattle; 2000. p.1756–61.
[22] Jenkins N, Allan R, Crossley P, Kirschen D, Strbac G. Embedded generation. London: IET; 2000.
[23] Hossain MJ, Pota HR, Ugrinovskii VA, Ramos RA. Simultaneous STATCOM and pitch angle control for improved LVRT capability of fixed-speed wind turbines. IEEE Transactions on Sustainable Energy 2010;1(3):142–51.
[24] IEEE task force on load representation for dynamic performance. Standard load models for power flow and dynamic performance simulation. IEEE Transactions on Power Systems 1995;10(3):1302–13.
[25] Hossain MJ, Pota HR, Ugrinovskii VA, Ramos RA. Voltage mode stabilisation in power systems with dynamic loads. Electrical Power and Energy Systems 2010;32:911–20.
[26] IEEE standard for interconnecting distributed resources with electric power systems. IEEE Std. 1547-2003.
[27] IEEE application guide for IEEE Std. 1547, IEEE standard for interconnecting distributed resources with electric power systems. IEEE Std. 1547.2–2008.
[28] Cutsem TV, Vournas C. Voltage stability of electric power systems. Boston/London/Dordrecht: Kluwer Academic Publishers; 2003.
[29] ABB power quality solutions. Product brochure: PCS100 STATCOM. Available: www.abb.com/powerquality.
[30] Molinas M, Are SJ, Undeland T. Low voltage ride through of wind farms with cage generators: STATCOM versus SVC. IEEE Transactions on Power Electronics 2008;23:1104–17.
[31] Xue D, Chen Y, Atherton DP. Linear feedback control: analysis and design with MATLAB. Philadelphia: Society for Industrial and Applied Mathematics (SIAM); 2007.
[32] Freitas W, Vieira JCM, Morelato A, da Silva LCP, da Costa VF, Lemos FAB. Comparative analysis between synchronous and induction machines for distributed generation applications. IEEE Transactions on Power Systems 2006;21(1):301–11.
[33] Civanlar S, Grainger JJ, Yin H, Lee SSH. Distribution feeder reconfiguration for loss reduction. IEEE Transactions on Power Delivery 1988;3(3):1217–23.